Decentralized Model Predictive Control of Electrical Power Systems

M. Kahl, T. Leibfried

***Abstract*—This paper presents an integral control strategy which integrates data from phase measurement units to damp inter-area oscillations. The proposed decentralized model predictive control method has one control unit for each controllable device (Generators, FACTS, HVDC) and coordinates their behavior after a fault. Each unit is designed by applying a systematic controller synthesis. The decentralized model predictive controller has a significantly improved dampening performance compared to a standard power system stabilizer. The stability and robustness can be evaluated. Furthermore, the control method also works with several transfer rates.**

***Keywords*: PSS, model predictive control, PMU, inter-area oscillation**

I. Introduction

THE growing demand for electrical power, the expansion of renewable energy sources (RES) and the hesitant extension of the power grid have increased the strain on the grid significantly. Consequently, transfer capabilities are very close to their limits and post-fault corrective actions are needed more often. With the rising number of RES the power system becomes more and more complex. Additionally, the amount of rotating mass decreases which has negative effects on grid stability.

The existing electrical power systems in Europe and North America have multiple monitoring systems at transmission level. However, the control systems of power plants rely only on local measurements. The control law is therefore not based on the overall grid state, but only on the measured terminal voltages and frequency deviations.

The proposed decentralized model predictive controller (dMPC) incorporates data from phase measurement units (PMU) into the control system. This concept is based on an analytical model, and hence inherently considers the stability and describes dynamical interaction between generators, power converters and grid dynamics.

Several power system stabilizer (PSS) design methods have been developed with significant effort. PSS methods can be divided into damping torque, frequency response and eigenvalue techniques. In [9] the damping torque concept has been developed, where the proportionality between electrical damping torque and speed perturbations is applied to damp the system. Whereas in [10] and [7] a robust, decentralized approach is proposed using linear matrix inequalities based on pole placement and H_∞ respectively. In [11] wide area dynamical information is integrated into the control system based on a selective modal performance index, damping inter-area modes. In [4] dMPC strategies have been formulated and applied to the control of the power system. The paper shows that the performance benefits obtained from MPC can be realized through dMPC for large scale systems.

Due to the decentralized structure of the MPC controller, an implementation of large systems becomes viable. Classical PSS depend only on local measurements. With PMU control methods, which rely not only on local measurements, but on several node voltages become feasible. Multi-Input, Multi-Output (MIMO) controllers account explicitly for couplings of the system and achieve an optimal control, considering all generators and power converters. Especially complex, coupled systems with several in- and outputs perform significantly better with a MIMO controller. dMPC control is based on MPC control, which is a MIMO controller with the described advantages. The presented dMPC control strategy achieves results very close to the global optimum for the following reasons. One decentralized control unit considers all state and input variables for the optimization. Every controller has the same global objective and considers the couplings of the entire system. The controller relies primarily on local measurements and uses global measurements when available. Thus, the approach does not assume a global sample rate.

This paper is organized as follows: The synchronous generator and dynamic network models are introduced. Based on the models, an overall system is formulated and the dMPC control theory is explained. The potential of the dMPC controller in comparison to PSS is demonstrated with simulation results for a 4 generator network.

II. Deployed Model

A. Generator Model

A generator model proposed by [3] is used with fluxes per second as state variables, where ψ_d and ψ_q are fluxes per second of the dq-components. ψ_{kd} and ψ_{kq1} denote the

Matthias Kahl is with the Department of Electric Energy Systems and High-Voltage Technology, Karlsruhe Institute of Technology, Karlsruhe, Germany (e-mail: Kahl@kit.edu)

Thomas Leibfried is with the Department of Electric Energy Systems and High-Voltage Technology, Karlsruhe Institute of Technology, Karlsruhe, Germany, e-mail: Thomas.Leibfried@kit.edu.

Paper submitted to the International Conference on Power Systems Transients (IPST2013) in Vancouver, Canada July 18-20, 2013.

fluxes per second of the damper windings. Furthermore, ψ_{fd} is the flux per second of the excitation. u_e denotes the terminal voltage and u_f the excitation voltage.

$$\begin{pmatrix} \psi_q \\ \psi_d \\ \psi_{kq1} \\ \psi_{fd} \\ \psi_{kd} \end{pmatrix}^{\bullet} = A_{gen}^{NL} \begin{pmatrix} \psi_q \\ \psi_d \\ \psi_{kq1} \\ \psi_{fd} \\ \psi_{kd} \end{pmatrix} + B_{gen}^{NL} \begin{pmatrix} u_e^r \\ u_f^r \end{pmatrix} \quad (1)$$

Only a symmetric operating mode is considered. The 0-component is hence omitted. The torque equation

$$\dot{\omega}_r = -\frac{\omega_b}{2H}\left(\underbrace{\left(i_q^r\,\psi_d - i_d^r\,\psi_q\right)}_{T_e} - T_m\right) \quad (2)$$

is used, where H is the coefficient of inertia and i_e^r is defined as following

$$i_e^r = \begin{pmatrix} i_d^r \\ i_q^r \end{pmatrix} = -\frac{1}{X_{ls}} \begin{pmatrix} \psi_d - \psi_{md} \\ \psi_q - \psi_{mq} \end{pmatrix}. \quad (3)$$

ψ_{md} and ψ_{mq} are the main fluxes per second and can be expressed as functions of the state variables in (1).
u_e^r and i_e^r are rotating with rotor speed ω_r and can be transformed to grid frequency with u_e^n, i_e^n. This is done using

$$T_\delta = \begin{pmatrix} \cos(\delta) & \sin(\delta) \\ -\sin(\delta) & \cos(\delta) \end{pmatrix}, \quad (4)$$

where δ is the rotor angle. The measurements of magnitude and phase can be transformed into dq-components rotating with grid frequency. Hence, dq-components rotating with rotor speed need to be transformed using (4). Substituting (4) into (1) leads to a nonlinear state space model, which depends on δ, ω and the fluxes per second due to (2).
The nonlinear model is linearized around an operating point

$$x_{gen} = \begin{pmatrix} \psi_{dq} & \psi_{kq1} & \psi_{fd} & \psi_{kd} & \delta & \omega \end{pmatrix}^T \quad (5)$$

$$\dot{x}_{gen} = A_{gen} x_{gen} + B_{gen1} u_f + B_{gen2} u_e^n \quad (6)$$

The output equation is a linearized form of (4) and (3).

$$i_e^n = C_{gen} x_{gen} \quad (7)$$

B. Network Model

The dynamic network model proposed by [1] and [2] is based on the node admittance matrix $i = Yu$. Y has the dimensions $(n \times n)$. To develop a dynamic model, each element of the admittance matrix is interpreted in Laplace space, which leads to the substitution $j\omega = s$,

$$\begin{pmatrix} i_F \\ i_N \end{pmatrix} = Y(s) \underbrace{\begin{pmatrix} u_F \\ u_N \end{pmatrix}}_{u} \quad (8)$$

where u_F and u_N denote the feeder and node voltages, respectively. The admittance matrix is based on Kirchhoff's current law as $i_N = 0$. Therefore, the voltage for every node can be calculated with the knowledge of i_F and a given impedance matrix where loads are included. The inverse of Y is defined as the adjugate divided by the determinant of Y.

$$u = Y^{-1}(s) i_F = Z(s) i_F$$
$$u = \frac{\mathrm{adj}(Y)}{\det(Y)} i_F \quad (9)$$

In order to obtain a polynomial denominator and numerator of minimal order, Z(s) needs to be extended by N_Δ. N_Δ is the product of the denominator of the lower triangular matrix, i.e. the denominator of Y_{ij} with (j > i).

$$u = \frac{\mathrm{adj}(Y)\, N_\Delta}{\det(Y)\, N_\Delta} i_F \quad (10)$$

The poles of Z(s) can be calculated with the determinant of Y, which are the eigenvalues of the system.

$$u = \frac{\mathrm{adj}(Y) N_\Delta}{V(s-\sigma_1)..(s-\sigma_{n_0})} i_F \quad (11)$$

Since the degree of the numerator is higher than that of the denominator, (11) can be decomposed into

$$u = \left(R + sL + \sum_{l=1}^{n_0} \frac{1}{s-\sigma_l} Z_l \right) i_F, \quad (12)$$

with a partial fraction decomposition, where n_0 is the number of poles. Moreover, Z_l can be decomposed into

$$Z_l = V_l \Lambda_l W_l, \quad (13)$$

where Λ_l are the eigenvalues of Z_l, V_l and W_l are left- and right-hand eigenvectors. The matrices Z_l have several properties as described by [1]. Since Y is symmetric and the properties of the adjugate are transferable to Z_l, the following properties can be formulated for Z_l:

If rank(Y(σ_l)) = n-1 $\Rightarrow$ rank(adj(Y(σ_l))) = 1
If rank(Y(σ_l)) < n-1 $\Rightarrow$ rank(adj(Y(σ_l))) = 0
Y is symmetric $\Rightarrow$ adj(Y) is symmetric

If Z_l is of rank 0, the decomposition (13) is not unique and Λ_l may set to zero.
Furthermore, if Z_l is of rank 1, the decomposition leads to Λ_l with only one non-zero element. Thus, Λ_l can be reduced to one element μ_l with the corresponding eigenvectors v_l and w_l.

$$Z_l = \mu_l v_l w_l \quad (14)$$

With (14) it is possible to formulate a state space model of minimal order, i.e. for every L-, C- element of the network only one state variable is introduced. In order to guarantee that the feeder currents i_F are state variables, it is necessary to feed the system using a series RL- impedance. This is always the case, when the in-feed is realized using a transformer.
The state variables are defined as

$$\zeta_l = \frac{v_l^T i_F}{s-\sigma_l} \tag{15}$$

and for complex eigenvalues as

$$\zeta_l = \frac{v_l^T i_F}{s-\sigma_l} + \frac{v_l^{*T} i_F}{s-\sigma_l^*} \tag{16}$$

$$\zeta_{l+1} = j\frac{v_l^T i_F}{s-\sigma_l} - j\frac{v_l^{*T} i_F}{s-\sigma_l^*}. \tag{17}$$

The state space equations in this case become

$$\dot{\zeta} = A_s\zeta + B_s i_F \tag{18}$$

$$u = C_s\zeta + R i_F + L\dot{i}_F, \tag{19}$$

where u indicates the feeder and node voltages.

$$A_s = \begin{pmatrix} \sigma_1 & & & & 0 \\ & \ddots & & & \\ & & \mathrm{Re}\{\sigma_l\} & \mathrm{Im}\{\sigma_l\} & \\ & & -\mathrm{Im}\{\sigma_l\} & \mathrm{Re}\{\sigma_l\} & \\ 0 & & & \ddots & \sigma_{n_0} \end{pmatrix} \tag{20}$$

$$B_s = \begin{pmatrix} v_1^T \\ \vdots \\ 2\mathrm{Re}\{v_l^T\} \\ -2\mathrm{Im}\{v_l^T\} \\ \vdots \end{pmatrix} \tag{21}$$

$$C_s = \begin{pmatrix} \mu_1 v_1 & \dots & \mathrm{Re}\{\mu_l v_l\} & \mathrm{Im}\{\mu_l v_l\} & .. \end{pmatrix} \tag{22}$$

A_s, B_s, C_s have the dimensions:

dim(A_s) = ($n_0 \times n_0$) dim(R) = ($n \times F$)

dim(B_s) = ($n_0 \times F$) dim(L) = ($n \times F$)

dim(C_s) = ($n \times n_0$)

where F is the number of feeds and n is the dimension of the node admittance matrix. Since $i_N = 0$, the matrices R- ,L- and B are not square, but have F columns.
After transforming (18) into dq-components we obtain

$$\dot{\zeta}_{dq} = A_N\zeta_{dq} + B_N i_{dq} \tag{23}$$

$$u_{dq} = C_N\zeta_{dq} + R_N i_{dq} + L_N\dot{i}_{dq}. \tag{24}$$

C. Overall Model

An overall model needs to be established to describe the interaction of several generators and the dynamic network model. Therefore, the feeding current of (24) is replaced by the generator output (7) and state equation (6).

$$u_{dq} = C_N\,\zeta_{dq} + R_N\,C_{gen}x_{gen} + L_N C_{gen}\,\underbrace{\dot{x}_{gen}}_{(6)} \tag{25}$$

The network and generator model are both dependent on u_{dq}. To link the corresponding terminal voltage with a feeding node $u_e = \chi\,u_{dq}$ is introduced, where $\chi = (E \;\; \underline{0})$. E is the 2x2 identity matrix. The identity matrix is placed at the positions which allow the selection of the terminal voltage u_e from all feeding voltages u_{dq} with the dimension $(2F \times 1)$.

$$u_e = \alpha\left(C_N\,\zeta + \nu\,x_G + L_N\,C_{gen}\,B_{gen1}\,u_f\right) \tag{26}$$

$$\alpha = (I - L_N\,C_{gen}B_{gen2}\,\chi)^{-1}$$

$$\nu = \left(R_N C_{gen} + L_N\,C_{gen}A_{gen}\right)$$

Substituting (26) into (6), (7) into (23) results in a coupled system (27) of generator and network states.

$$\begin{pmatrix} x_{gen} \\ \zeta_{dq} \end{pmatrix}^{\bullet} = \begin{pmatrix} A_{gen} + B_{gen2}\,\chi\,\alpha\,\nu & B_{gen2}\,\chi\,\alpha\,C_N \\ B_N C_{gen} & A_N \end{pmatrix}\begin{pmatrix} x_{gen} \\ \zeta \end{pmatrix} + \begin{pmatrix} B_{gen1} + B_{gen2}\,\chi\,\alpha\,L_N C_{gen}\,B_{gen1} \\ 0 \end{pmatrix} u_f \tag{27}$$

The coupled system of n generators and one network can be deduced with the same procedure. (29) is a continuous system suitable for controller synthesis. The output equation is denoted with (26) and an identity matrix is included that defines ω as an output variable. The optimal stabilizing trajectory u_{stab} for the system is calculated with the measurements from u_{dq} and ω taken from each in-feed. u_{stab} is added to an IEEE type 1 voltage regulator that is also included in the model.

$$\begin{pmatrix} x_{gen-1} \\ \vdots \\ x_{gen-n} \\ \zeta_{dq} \end{pmatrix}^{\bullet} = A_{tot}\begin{pmatrix} x_{gen-1} \\ \vdots \\ x_{gen-n} \\ \zeta_{dq} \end{pmatrix} + B_{tot}\begin{pmatrix} u_{stab1} \\ \vdots \\ u_{stab\,n} \end{pmatrix} \tag{28}$$

$$\begin{pmatrix} u_{dq1} \\ \vdots \\ \omega_1 \\ \vdots \end{pmatrix} = C_{tot}\begin{pmatrix} x_{gen-1} \\ \vdots \\ x_{gen-n} \\ \zeta_{dq} \end{pmatrix} + D_{tot}\begin{pmatrix} u_{stab1} \\ \vdots \\ u_{stab\,n} \end{pmatrix} \tag{29}$$

Since $D_{tot} \approx 0$, D_{tot} has a very small influence on the system behavior. Thus, D_{tot} is omitted in the following. With (29) a model is introduced which describes the coupling between generator states and network states. Model predictive control is a time discrete control method. Therefore, (28) and (29) are transformed into the time discrete model (30).

1) Partitioned Model

Model partitions can be chosen arbitrarily, however in case of an electrical power system each generator is summarized as one sub-model and the network is also compiled into one sub-model. Each generator sub-model can be controlled via u_{stab}.

$$x^{(k+1)} = A\,x^{(k)} + B\,u^{(k)} \qquad y^{(k)} = C\,x^{(k)} \tag{30}$$

$$A = \begin{pmatrix} A_{11} & \cdots & A_{1M} \\ \vdots & \ddots & \vdots \\ A_{M1} & \cdots & A_{MM} \end{pmatrix}$$
$$B = \begin{pmatrix} B_{11} & \cdots & B_{1M} \\ \vdots & \ddots & \vdots \\ B_{M1} & \cdots & B_{MM} \end{pmatrix}$$
$$C = \begin{pmatrix} C_{11} & \cdots & C_{1M} \\ \vdots & \ddots & \vdots \\ C_{M1} & \cdots & C_{MM} \end{pmatrix} \tag{31}$$
$$x^{(k)} = \left(x_1^{(k)} \quad \cdots \quad x_M^{(k)}\right)^T$$
$$u^{(k)} = \left(u_1^{(k)} \quad \cdots \quad u_M^{(k)}\right)^T$$
$$y^{(k)} = \left(y_1^{(k)} \quad \cdots \quad y_M^{(k)}\right)^T$$

Any other controllable device, such as FACTs or HVDC can be modeled and included in a subsystem as well.

III. Control Scheme

Conventional PSS have a decentralized control structure, and rely only on local measurements. The network and generator states of the deduced model (30) are heavily coupled and thus a MIMO controller has a better performance than a PSS. An implementation of a classical MIMO controller, with a central structure and one sample rate, will undoubtedly fail in practical applications, due to the spatially distributed nature of power systems. However, dMPC is an approach to implementing a controller that achieves results very close to its central counterpart and fulfills the conditions created by a real world system.

The proposed control method shown in figure (1) has the following structure: A dMPC controller is implemented for each controllable device. Each controller works with two sample rates. The method is also extendable to several sample rates without any disadvantages. The primary rate Ts_h is given by the local measurement system and the secondary sample rate by the global measurement Ts_l system. Ts_h is assumed to be an integer multiple of Ts_l, therefore is $r \cdot Ts_h = Ts_l$ with $r \in \mathbb{N}$.

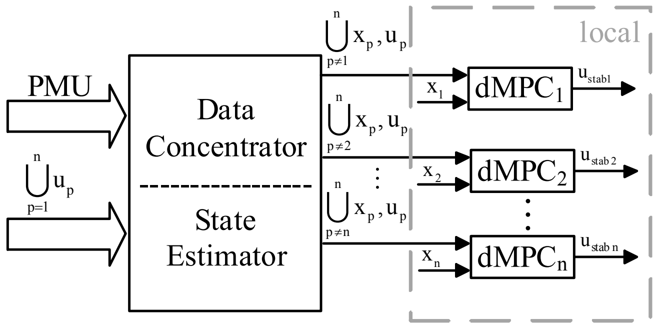

Figure 1: Control scheme with decentralized control units, one data concentrator state estimator

As indicated in [8], it is advantageous to position the PMUs at the in-feed nodes, involved in frequency and/or voltage control. Every major feeding node has one PMU available, where $\underline{U}$, $\underline{I}$ and ω are measured, thus enabling the calculation of the local generator states. Since dMPC controller and PMU are located in proximity of each other a high transfer rate of Ts_h is assumed.

All PMUs transmit their data to a data concentrator, which preprocesses the data for the dynamic state estimator. The state estimator also includes a state space model and estimates all state variables of the overall model (30). The trajectories of the dMPC controllers u need to be exchanged as well. The estimates $\hat{x}$ are transmitted to the dMPC omitting the available local measurements. For the procedure of transmitting PMU measurements, estimation and transmission of $\hat{x}$ and u a low transfer rate of Ts_l is assumed. Only one data concentrator is needed for the proposed control scheme. A detailed example of the control structure and data transmissions for a benchmark model is depicted in Figure (2). The control variables are u_{dq} and ω for each generator.

IV. Feasible Cooperation Model Predictive Control

A model predictive controller anticipates the plant behavior with a model over a prediction horizon of N time steps. The MPC method is based on [4], where a detailed derivation can be found.

The discrete model (30) is successively inserted into itself i.e. (32) into (33). This is done to demonstrate the procedure for two time steps. p always denotes variables of external subsystems and j always denotes variables of the own subsystem.

$$x_j^{(k+1)} = A_{jj}x_j^{(k)} + B_{jj}u_j^{(k)} + \sum_{p\neq j}^{M} A_{jp}x_p^{(k)} + B_{jp}u_p^{(k)} \tag{32}$$

$$x_j^{(k+2)} = A_{jj}x_j^{(k+1)} + B_{jj}u_j^{(k+1)} + \sum_{p\neq j}^{M} A_{jp}x_p^{(k+1)} + B_{jp}u_p^{(k+1)} \tag{33}$$

Since $r \cdot Ts_h = Ts_l$, u_p and x_p are updated only at every (r-1) th time step of the primary sample rate Ts_h. Hence,

$$x_p^{(k+r-1)} = \ldots = x_p^{(k)} \tag{34}$$

$$u_p^{(k+r-1)} = \ldots = u_p^{(k)} \quad (35)$$

which expands (33) to

$$x_j^{(k+2)} = A_{jj}^2 x_j^{(k)} + A_{jj}B_{jj}u_j^{(k)} + B_{jj}u_j^{(k+1)} + \sum_{p\neq j}^{M}(A_{jj}A_{jp} + A_{jp})x_p^{(k+1)} + (A_{jj}B_{jp} + B_{jp})u_p^{(k+1)}$$

A general predictive form of a model for N time steps Ts_h, which depends only on $\bar{u}$ and the current state $x^{(k)}$ is

$$\bar{x}_j = \sum_{p=1}^{M}\left[E_{jp}\bar{u}_p + f_{jp}x_p^{(k)}\right], \quad (36)$$

with

$$\bar{x}_j = \left(x_j^{(k+1)} \quad x_j^{(k+2)} \quad \cdots \quad x_j^{(k+N)}\right)^T \quad (37)$$

$$\bar{u}_j = \left(u_j^{(k+1)} \quad u_j^{(k+2)} \quad \cdots \quad u_j^{(k+N)}\right)^T \quad (38)$$

for the subsystem j. The matrices E and f are defined in the appendix. Since the existing problem is an output regulator problem with the control variables u_{dq} and ω, the output equation over the prediction horizon is needed. The output j is coupled with all subsystems

$$\bar{y}_j = \sum_{i=1}^{M}\tilde{C}_{ji}\bar{x}_i. \quad (39)$$

The MPC controller calculates the optimal actuating variable considering the cost function

$$V_j = \sum_{s=1}^{M}\omega_{js}\left[\|\bar{y}_s - \tau_s\|_{\bar{Q}}^2 + \|\bar{u}_s\|_{\bar{R}}^2\right]. \quad (40)$$

Cooperation of the dMPC controllers is needed to achieve system wide objectives. Therefore, the overall system influence and the objectives of all subsystems are incorporated intoV_j, the cost function of one subsystem j. w_{js} is a weighting term for each subsystem with $\sum_s w_{js} = 1$ and $w_{js} > 0$. τ_s is the set point for each subsystem and Q, R are positive-definite weighting matrices.

A quadratic cost function was taken for this example. Complex cost functions as indicated in [11], could be advantageous. The matrix $\tilde{C}_{ji}$ is also defined in the appendix. Substituting (36) into (39) and the resulting equation into (40) formulates a PQ-problem. V_j is only optimized for $\bar{u}_j$.

$$V_j = \min_{\bar{u}_j}\frac{1}{2}\bar{u}_j^T\Phi_j\bar{u}_j + (K_{MPC,j}x + \sum_{p\neq j}W_{MPC,jp}\bar{u}_p)^T\bar{u}_j \quad (41)$$

To calculate the optimal solution for a trajectory $\bar{u}_{opt,j}$, equation (41) is differentiated with respect to $\bar{u}_j$ and set to zero.

$$\frac{dV_j}{d\bar{u}_j} = (K_{MPC,j}x + \sum_{p\neq j}W_{MPC,jp}\bar{u}_p)^T + \Phi_j\bar{u}_j = 0 \quad (42)$$

$$\bar{u}_{opt,j} = -\Phi_j^{-1}(K_{MPC,j}x + \sum_{p\neq j}W_{MPC,jp}\bar{u}_p)^T \quad (43)$$

Φ_j, $K_{MPC,j}$ and $W_{MPC,jp}$ are defined in the appendix. The implemented dMPC procedure does not explicitly account for constraints such as the rate of change or saturation effects. Therefore, a static control matrix can be calculated, which has several inherent advantages.

- The optimization can be calculated offline
- No iterative approach
- Stability and robustness analysis is possible

A. *Stability assessment*

The stability of the system can be calculated with

$$x^{(k+1)} = Ax^{(k)} + Bu_{opt}^{(k)} \quad (44)$$

The system is defined according to (30) and (31). Substituting (43) into (44) leads to

$$(A - B\Phi^{-1}K_{MPC})x^{(k)}. \quad (45)$$

The eigenvalues of (45) need to be stable, furthermore robustness properties can be analysed according to [13].

V. Simulation Results

A 4 generator benchmark model according to [5] is chosen to demonstrate the performance of the developed dMPC approach. The network including communication and control structure is depicted in Figure (2). Each feeding node is equipped with a PMU. Due to the proximity of the PMU to the corresponding dMPC a high transmission rate of Ts_h = 50ms is assumed. The PMU data and the trajectories of each dMPC are also transmitted through a data concentrator to the state estimator. A Kalman-Bucy Filter is used for the estimation. By applying (29), the filter estimates all state variables x. As indicated in Figure (1) all state variables, except for those x_j locally available, are transferred to the corresponding dMPC controller. In addition, all trajectories u need to be exchanged. The procedure of data transmission and state estimation is more time consuming. The transfer rate of external signals Ts_l is allowed to be four times lower than the primary transfer rate Ts_h. (Ts_l =200ms)

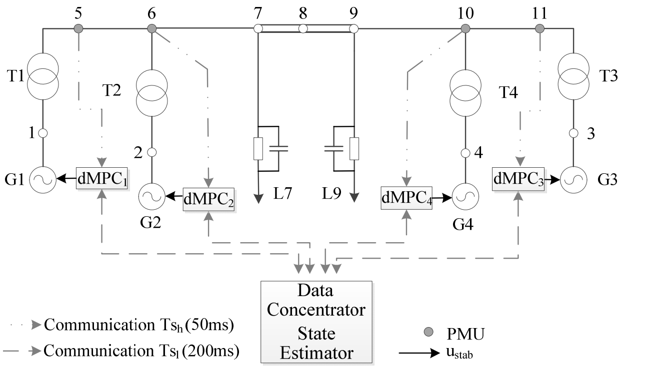

Figure 2: Network with dMPC control, communication, data concentrator and state estimator

The stabilizing signal u_{stab} from each dMPC unit is added to the excitation control.

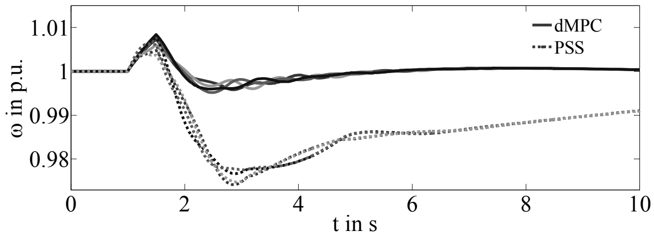

Figure 3: ω of dMPC controlled system in comparison to PSS after a 500 ms short circuit

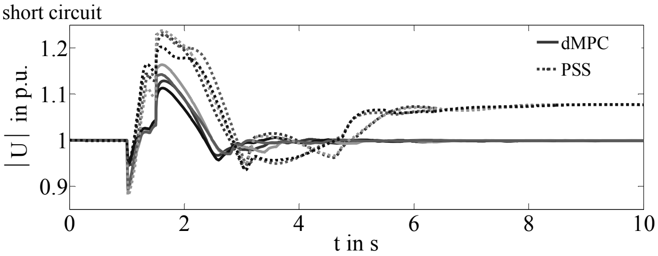

Figure 4: |U| of dMPC controlled system in comparison to PSS after a 500 ms short circuit

Figure 3 shows the rotor speed and Figure 4 shows the magnitude of the terminal voltages of all generators. The simulation results created with the dMPC procedure (continuous line) are compared to a MB-PSS IEEE® type PSS4B according to IEEE Std 421.5 (dotted line). After one second of simulation time a 3-phase short circuit occurs at node 8 for 500 ms. dMPC and PSS are able to stabilize the system. However, as depicted in Figures 3 and 4 the time evolution of the rotor speed and voltage magnitude of the dMPC controlled system are significantly better than the PSS controlled system. The maximum rotor speed deviation of the dMPC controlled system is 0.005 p.u. compared to 0.025 p.u. for the PSS controlled system. After just 2.5 s the terminal voltage of the dMPC controlled system is equal to the set point. The PSS needs 5.5 s to damp the oscillation, and needs 28.5 s to return the terminal voltage back to its set point.
Moreover, simulation results show that if the transfer rate is chosen such that $Ts_l = Ts_h = 0.05$ s, the dynamic performance can be further improved. Furthermore, if the transfer rate is chosen to $Ts_l = Ts_h = 0.2$ s, the system cannot be stabilized.

VI. Conclusion

The paper presents a novel approach to systematically integrate PMU-data and coordinate a large number of actuating hardware (Generators, FACTS, HVDC) even when several transfer rates are involved. The optimal trajectories for each control variable are calculated in order to damp inter-area oscillations. Each controller complies with the global objective. Hence, the dMPC approach has a dynamic performance close to a central MPC [4]. The method accounts for several transfer rates. The performance is significantly better compared to a MB-PSS, and thus the dMPC approach improves reliability and the operational flexibility.

Furthermore, a novel model for power systems including grid dynamics has been established. Since inter-area oscillations appear at frequencies around 0.01 – 3 Hz, a static model operating at grid frequency cannot describe the phenomena correctly. A dynamic grid model is able to describe transients over the whole spectrum.

VII. Appendix

The following matrices are defined:

$$\bar{E}_{jp} = \begin{pmatrix} B_{jp} & 0 & \cdots & \cdots & 0 \\ A_{jj}B_{jp} & B_{jp} & 0 & \cdots & 0 \\ \vdots & \ddots & \ddots & \ddots & \vdots \\ A_{jj}^{N-1}B_{jp} & \cdots & \cdots & \cdots & B_{jp} \end{pmatrix} \tag{46}$$

$$\bar{f}_{jj} = \begin{pmatrix} A_{jj} \\ A_{jj}^2 \\ \vdots \\ A_{jj}^N \end{pmatrix} \tag{47}$$

$$\bar{f}_{jp} = \begin{pmatrix} A_{jp} \\ A_{jj}A_{jp} \\ \vdots \\ \sum_{j=N-r}^{N-1} A_{jj}^{N-1}A_{jp} \end{pmatrix} \tag{48}$$

$$h_{(j,p)} = \begin{pmatrix} 0 & 0 & \cdots & \cdots & 0 \\ A_{jp} & 0 & 0 & \cdots & 0 \\ \vdots & \ddots & \ddots & \ddots & \vdots \\ A_{jj}^{N-2}A_{jp} & A_{jj}^{N-3}A_{jp} & \cdots & \cdots & 0 \end{pmatrix} \tag{49}$$

The variables u_p and x_p of all external subsystems are only updated every r-1 time steps, the derivation of [12] is modified.

$$O_{(j,r\cdot p+1)} = \sum_{z=1}^{r} \bar{E}_{(j,r\cdot p+z)} \tag{50}$$

$$\bar{g}_{(j,r\cdot p)} = \sum_{z=0}^{r-1} h_{(j,p\cdot r+z)} \tag{51}$$

Elements of O and $\bar{g}$ which are not defined by (50) and (51), respectively, are zero. For the system of equations (32), (33) and following time steps

$$\tilde{A}\tilde{x} = \tilde{E}\tilde{u} + \tilde{G}x(k) \tag{52}$$

equation (52) can be formulated with (53)-(57).

$$\tilde{G} = \begin{pmatrix} \bar{f}_{11} & \cdots & \bar{f}_{1M} \\ \vdots & \ddots & \vdots \\ \bar{f}_{M1} & \cdots & \bar{f}_{MM} \end{pmatrix} \tag{53}$$

$$\tilde{E} = \begin{pmatrix} \overline{E}_{11} & O_{12} & \cdots & O_{1M} \\ O_{21} & \overline{E}_{22} & \cdots & O_{2M} \\ \ddots & \ddots & \ddots & \ddots \\ O_{M1} & \cdots & \cdots & \overline{E}_{MM} \end{pmatrix} \tag{54}$$

$$\tilde{A} = \begin{pmatrix} I & -\overline{g}_{12} & \cdots & -\overline{g}_{1M} \\ -\overline{g}_{21} & I & \cdots & -\overline{g}_{2M} \\ \ddots & \ddots & \ddots & \ddots \\ -\overline{g}_{M1} & \cdots & \cdots & I \end{pmatrix} \tag{55}$$

$$\tilde{x} = \begin{pmatrix} \overline{x}_1 & \overline{x}_2 & \cdots & \overline{x}_M \end{pmatrix}^T \tag{56}$$

$$\tilde{u} = \begin{pmatrix} \overline{u}_1 & \overline{u}_2 & \cdots & \overline{u}_M \end{pmatrix}^T \tag{57}$$

Equation (52) solved for $\tilde{x}$, leads to the predictive model (36)
.

$$E = \tilde{A}^{-1}\tilde{E} \tag{58}$$

$$f = \tilde{A}^{-1}\tilde{G} \tag{59}$$

$$\tilde{C}_{ji} = \begin{pmatrix} C_{ji} & \cdots & 0 \\ \vdots & \ddots & \vdots \\ 0 & \cdots & C_{ji} \end{pmatrix} \tag{60}$$

dMPC controller:

$$\Phi_j = \left[\omega_{jj} R_j + \sum_{s=1}^{M} \left[\sum_{i=1}^{M} (\tilde{C}_{si} E_{ij})^T \omega_{js} Q_s \sum_{i=1}^{M} (\tilde{C}_{si} E_{ij}) \right] \right] \tag{61}$$

$$K_{MPC,j} x = \sum_{s=1}^{M} \sum_{i=1}^{M} (\tilde{C}_{si} E_{ij})^T \omega_{js} Q_s \left(\sum_{i=1}^{M} \tilde{C}_{si} \sum_{p=1}^{M} \left[f_{ip} x_p \right] \right)$$

$$\sum_{p \neq j} W_{MPC,jp} \overline{u}_p = \sum_{s=1}^{M} \sum_{i=1}^{M} (\tilde{C}_{si} E_{ij})^T \omega_{js} Q_s \sum_{i=1}^{M} \tilde{C}_{si} \left[\sum_{p \neq j}^{M} \left[E_{ip} \overline{u}_p \right] \right]$$

VIII. References

[1] G. Hirsch, „Semianalytische Simulation von systemimmanenten elektromechanischen Pendelschwingungen in Verbundnetzen," 2003.

[2] O. Lotter, „Natural Minimal Set of State Equations of Linear Power Grid," Electrical Engineering, Springer, Bd. 5, pp. 405-409, 2007.

[3] P. Krause, Analysis of electric machinery and drive systems, N. Piscataway, Hrsg., IEEE Press, 2002.

[4] A. Venkat, I. Hiskens, J. Rawlings und S. Wright, „Distributed MPC Strategies With Application to Power System Automatic Generation Control," Control Systems Technology, IEEE Transactions on, Bd. 16, Nr. 6, pp. 1192-1206, nov. 2008.

[5] P. Kundur, Power system stability and control, N. York, Hrsg., McGraw, 1994.

[6] I. Kamwa, R. Grondin und Y. Hebert, „Wide-area measurement based stabilizing control of large power systems-a decentralized/hierarchical approach," Power Systems, IEEE Transactions on, Bd. 16, Nr. 1, pp. 136-153, feb 2001.

[7] B. Pal und B. Chaudhuri, Robust Control in Power Systems, N. New York, Hrsg., Springer, 2005.

[8] M. Glavic, T. Van Cutsem, "Investigating State Reconstruction from Scarce Synchronized Phasor Measurements," Proc. IEEE PowerTech, Trondheim, Norway, June 2011.

[9] M. Gibbard, D. Vowles und P. Pourbeik, „Interactions between, and effectiveness of, power system stabilizers and FACTS device stabilizers in multimachine systems," Power Systems, IEEE Transactions on, Bd. 15, Nr. 2, pp. 748-755, may 2000.

[10] R. Ramos, L. Alberto und N. Bretas, „A new methodology for the coordinated design of robust decentralized power system damping controllers," in Power Engineering Society General Meeting, 2004. IEEE, 2004.

[11] I. Kamwa, R. Grondin und Y. Hebert, „Wide-area measurement based stabilizing control of large power systems-a decentralized/hierarchical approach," Power Systems, IEEE Transactions on, Bd. 16, Nr. 1, pp. 136-153, feb 2001.

[12] A. N. Venkat, "Distributed model predictive control: Theory and applications," Ph.D. dissertation, University of Wisconsin-Madison, Wisconsin-Madison, USA, 2006.

[13] Lunze, Jan. *Robust Multivariable Feedback Control*. New York. Prentice Hall, 1989